

Semi-analytical Industrial Cooling System Model for Reinforcement Learning

Yuri Chervonyi^{*,1}, Praneet Dutta^{*,1}, Piotr Trochim², Octavian Voicu¹, Cosmin Paduraru¹, Crystal Qian^{2,3}, Emre Karagozler¹, Jared Quincy Davis¹, Richard Chippendale⁴, Gautam Bajaj³, Sims Witherspoon¹ and Jerry Luo¹

^{*}Equal contributions, ¹DeepMind, ²Work done at DeepMind, ³Google, ⁴Work done at COMSOL

We present a hybrid industrial cooling system model that embeds analytical solutions within a multi-physics simulation. This model is designed for reinforcement learning (RL) applications and balances simplicity with simulation fidelity and interpretability. The model’s fidelity is evaluated against real world data from a large scale cooling system. This is followed by a case study illustrating how the model can be used for RL research. For this, we develop an industrial task suite that allows specifying different problem settings and levels of complexity, and use it to evaluate the performance of different RL algorithms.

1. Introduction

1.1. Background and Motivation

Industrial systems account for 54% of global energy usage [6] and 24% of global net anthropogenic Greenhouse Gas (GHG) emissions. The latter percentage rises to 34% if indirect emissions from energy are included, which would make industrial systems the highest emitting sector [35]. Due to increasing global demand for the products and services enabled by industrial systems, emissions from this sector will continue to rise [26]. However, there is strong evidence that interventions such as reduction in energy use per unit of output [38], lightweight designs and extended product lifetimes can facilitate critical emissions reductions across industrial systems [21]. Yet, optimizing industrial systems is not straightforward; subsectors such as metals, chemicals, waste and cement require customized approaches accounting for different materials, processes and facility configurations.

Recent work has shown that reinforcement learning can be leveraged to efficiently control and optimize industrial processes (e.g. see [37, 39]). Among these processes, *cooling*/heating has been the main focus for many applied researchers due its wide usage in residential and commercial buildings, automobiles, industrial plant machinery, nuclear reactors, and many other types of machinery. Examples of applying RL in real cooling/heating systems include reducing energy consumption for cooling Google data centers by 40% [2] and controlling the HVAC systems, hot water tank and heat pumps in residential [23] and industrial facilities [12, 40, 20].

However, applying RL in live facilities comes with technical challenges, such as:

- *Limited exploration*: During exploration, the agent must act cautiously to avoid real-world consequences such as overheating a critical facility. The agent cannot explore all combinations of the state and action space, resulting in low-variance data. Furthermore, explore-exploit schedules must be negotiated with the facility, often with the motivation for the agent to exploit sooner rather than later.
- *Generalization*: Although many industrial facilities are similar, policies trained on one facility may not generalize to another facility due to slight differences in the input feature space. Solutions are not robust to different equipment conditions, weather patterns, and other sources of variance, as training is limited to experiences with a singular system during a fixed amount of real time interactions.

- *Sample efficiency*: In live facilities, the agent interacts with the environment and receives information at coarse frequencies such as 5 minutes or an hour; this limits the amount of data that can be used for training and also slows the process of validating existing models. From an algorithmic perspective, we are constrained to approaching this problem with sample-efficient algorithms.
- *Infrastructure and stakeholder management*: Interacting with a live facility requires significant additional engineering effort, including developing a shared data schematic and data transfer API with the facility partner, writing custom logic to integrate facility-specific features, and ensuring reliability and availability during deployment.

With these challenges in mind, we present a novel semi-analytical simulation model of an industrial cooling facility, developed specifically for reinforcement learning applications. Interacting with a simulator rather than a live facility greatly increases the amount of available data and allows the agent to explore a broader action space safely. We provide a set of analytical equations as well as the description of how to embed them into a multi-physics simulation software. We hope that this will be a useful blueprint for practitioners who want to improve industrial cooling system efficiency using RL.

In order to allow us to create agents that generalize well, we also provide the high level design for an Industrial Task Suite (ITS) that allows us to specify different RL tasks based on the simulator. ITS can be used to generate a curriculum of scenarios and defines highly parameterized facility configurations to enable flexible experimentation and the development of generalizable agents.

1.2. Related Work

1.2.1. Simulation

There are several tools offered for developing simulations for optimizing industrial systems and processes. Among such tools, EnergyPlus [14] is a popular open-source library for whole-building energy simulations. It is used by many researchers, especially for the RL applications [13, 30, 20]. Although it provides full-featured functionality, there are fidelity limitations that can be crucial when simulating real-world environments [25, 32].

1.2.2. Optimization Research

Work in the domain of simulation-enabled industrial system optimization research can broadly be segmented into those primarily addressing questions pertaining to data, infrastructure, and methods. Nweye et al. [33] has probed challenges around safety-critical building control and offline training, arguing that the sequence of operations policy used to generate offline trajectory data has a dramatic effect on the downstream performance of the associated offline RL agents. With regards to infrastructure, [20] proposes a scheme for weaving together popular free and open source tools to create common building control research infrastructure and environments. It illustrates a scheme for framing HVAC control as a Deep RL problem using OpenAI gym [10], EnergyPlus [14], and Ray RLlib [27]. The authors overlay real-world historical weather data from Toronto, Canada, and simulate a year's worth of weather dynamics, producing ablations to show the impact of weather, and energy-temperature penalty coefficients. In terms of the methods, many approaches have been proposed for energy savings and temperature control. For example, Gao et al. [17] explored the use of a Deep Deterministic Policy Gradients algorithm (DDPG) [28]; Zhang et al. [40] considered the Asynchronous Advantage Actor Critic (A3C) [29]. Other adjacent works explore applications of deep RL in other industrial control constrained optimization settings, such as assembly line control [37] and combustion control [39], proposing parallel agent training schemes to optimize throughput and mitigate simulation step-time limitations.

1.3. Summary of Results

Our main contributions include:

- Equations and design for our *Semi-analytical Industrial Cooling System Model*, a simulation of a large cooling facility that combines analytical solutions with a multi-physics simulation software (Section 2.2). The model’s fidelity is verified against real-world data from a large commercial cooling facility in the United States (Section 2.3).
- Design for the *Industrial Task Suite* (ITS), a framework for RL research in the domain of industrial systems (Section 3.1). Although we primarily use it for the industrial cooling applications, several other use-cases are presented in Appendix B. ITS is designed to allow more granular configurability of environments compared to the available task suites (such as the DeepMind Control Suite [36]); specifically, allowing the combination of independently-defined noise, constraints, scenarios, tasks and simulators for modelling industrial problems.
- *Tasks* for industrial cooling systems categorized by their perceived complexity (Section 3.2). We also show how to define other new tasks using the capabilities of the ITS.
- *RL Agents Benchmarks* on these tasks (Section 3.4).

2. Industrial Cooling System Simulation

2.1. Chilled Water Plant System Overview

A cooling system is an apparatus employed to keep the temperature of a structure or device from exceeding limits imposed by needs of safety and efficiency [1]. Cooling systems use air or a liquid as a medium to absorb heat. Many applications use water because it has a high boiling point and specific heat. In the following sections, we focus on chilled water plants, cooling systems that leverage water-cooled pipelines.

A chilled water plant system is depicted on Figure 1. These systems are typically divided into two broader halves. The chilled water side extracts heat from the building and is responsible for cooling the rooms, keeping them within the desired temperature range. The condenser water side interacts with the outside environment and, in turn, extracts heat from the chilled water side. The flow of water is regulated through pumps on both sides. No water mass is exchanged between the loops, being restricted to heat transfer via conduction and convection. The cooling process can be achieved in the cooling tower by the latent heat of evaporation and the chillers via the vapor compression cycle.

Chilled water plant systems use evaporative cooling, in which highly energetic water molecules are evaporated from the surface, resulting in reduced temperature for the remaining water [19]. There are two types of temperature that are important in these cooling systems: *dry bulb temperature* and *wet bulb temperature*. Dry bulb temperature is measured by a regular thermometer, by exposing it to the stream of air while shielding it from radiation and moisture. Wet bulb temperature is the lowest possible temperature of water that can be achieved just by the evaporation of water. This can be measured by a thermometer covered in the water-soaked cloth (wet-bulb thermometer), over which air is passed. Dry bulb temperature and wet bulb temperature can be used to calculate the relative humidity of air.

The rate of cooling is controlled by setting various system parameters known as *setpoints*, such as temperature, pressure, fluid flow rates etc. Industrial cooling systems are typically controlled by a Building Management System (BMS), a heuristic-based policy that operates on these setpoints to keep the building at a safe and comfortable desired temperature. A low level proportional–integral–derivative (PID) controller changes an actuator parameter to minimize the delta between this desired setpoint recommendation and a measured sensor reading (see Figure 2). This setup, controlling setpoints for multi-objective optimization subject to constraints, lends itself well to reinforcement-learning approaches.

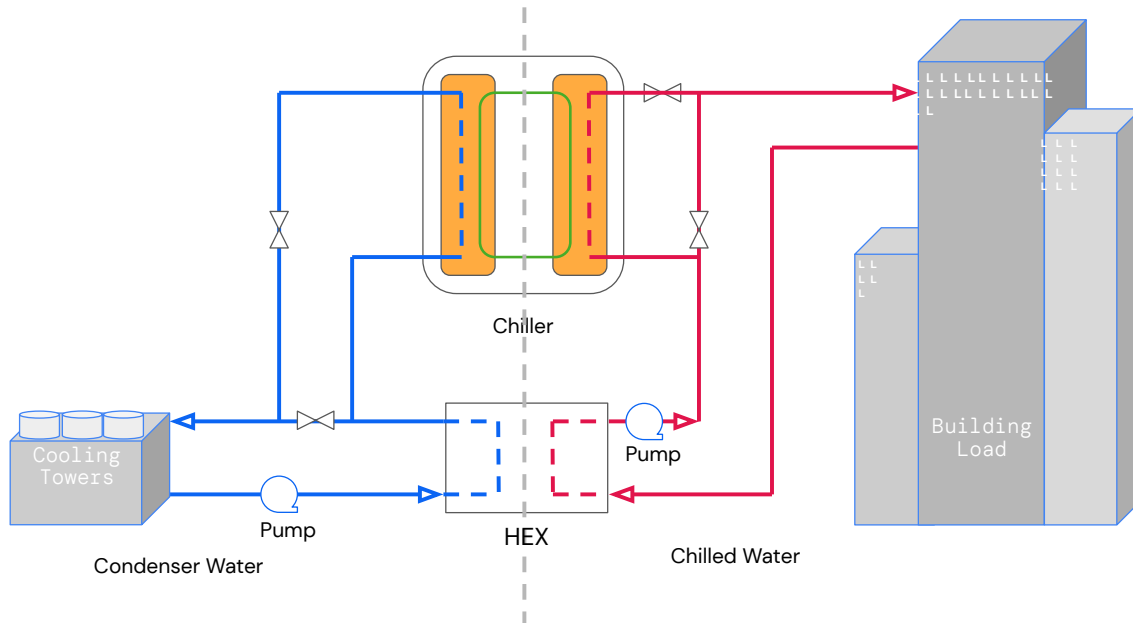


Figure 1 | A high level overview of a typical chilled water plant system. The main components include one or several chillers, a heat exchanger (HEX), pumps, cooling towers. Building load is heat transferred through the building envelope (walls, roof, floor, windows, doors etc.) and heat generated by occupants, equipment, and lights.

2.2. Semi-Analytical Simulation Model

We leverage a multi-physics simulator software (COMSOL) for modeling fluid and heat transfer across the system¹. The main components of our cooling system are (see Figure 1):

- Chillers.
- Cooling Towers.
- Chilled Water Pump Bank.
- Condenser Water Pump Bank.
- Air Handling Unit.
- Heat Exchanger.
- PID controllers.
- Valves, bends, friction loss parameters of the systems.

Our design goal is to balance simplicity with simulation fidelity and interpretability. We leverage a simplified pipe-flow module for modeling the fluid dynamics, which turns the meshed finite element analysis into a 2D curve, improving computational efficiency for 3D pipes with a finite diameter. We aim to model a large-scale industrial system where this approximation would be a reasonable assumption. Specifically, the pipe length to diameter ratio is large enough for the flow inside each pipe segment to be considered fully-developed. We utilize additional libraries for modeling the heat exchanger and PID controls, which controls components such as the temperature (via the compressor), pressure and flow rate (via the pumps) across the fluid loops. External weather conditions such as the dry bulb temperature, wet bulb temperature, relative humidity and the building load profile form a critical aspect of the system; we simulate these using public historical weather databases. Finally,

¹This setup could be replicated by any applicable fluid dynamics simulator

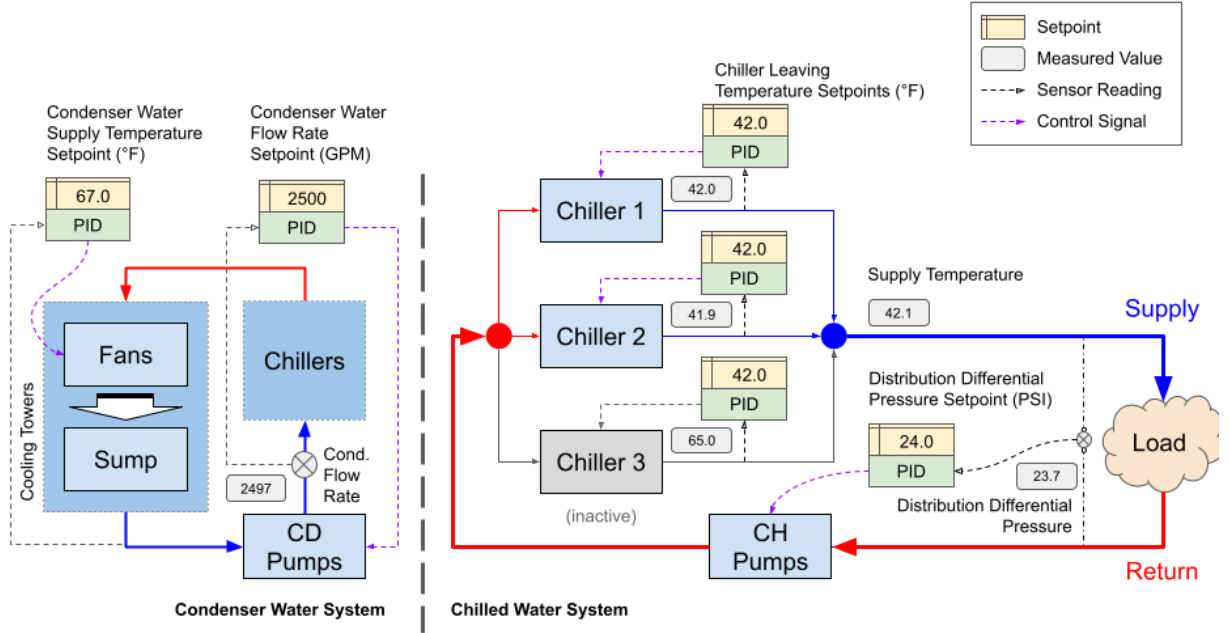


Figure 2 | The detailed overview of a chilled water plant system, including the most important setpoints that can be controlled to achieve the required temperature. Here we see multiple chillers arranged in parallel to handle various external conditions. Unlike a system presented on Figure 1, this design does not include a heat exchanger.

chillers, cooling towers and pump banks are described via analytical solutions that have been verified using data from a real-world facility. Next, we discuss these solutions in detail.

Chiller and the improved Gordon-Ng model For the chiller model we start with [16], where the canonical Gordon-Ng model [18] was simplified and improved. In this approximation, the chiller is represented via a simple vapor-compression cycle (see Figure 3). The laws of thermodynamics applied to this cycle under several assumptions, such as steady state, ignoring losses, etc (for the details see [16]), give:

$$W_{comp} = \frac{-DQ_{ev}^2 - CQ_{ev} - BQ_{ev} + A}{DQ_{ev} + C}, \quad (1)$$

$$Q_{ev} - Q_c + W_{comp} + Q_{LT} = 0, \quad (2)$$

$$Q_{ev} = C_{ch}(T_{chi} - T_{cho}), \quad (3)$$

$$Q_c = C_{cw}(T_{ci} - T_{co}). \quad (4)$$

Here W_{comp} is the chiller compressor power. Q_{ev} is the cooling load, the heat removed from the building through water flow. Q_c is the removed heat in the condenser. Q_{LT} is a total heat loss. T_{chi} and T_{cho} are the evaporator inlet and outlet temperatures. T_{ci} and T_{co} are the condenser inlet and outlet temperatures. $C_{ch} = \dot{m}_{ch}c_{ch}$ is the thermal capacitance of cooling water (kW/K) with \dot{m}_{ch} as a mass flow rate (kg/s) and c_{ch} water specific heat capacity. A, B, C, D are constants that encode various other quantities, the exact expressions for them can be found in [16]. As suggested in [16], one can estimate values for these constants upon actual measured values for the chiller.

If we neglect all heat losses Q_{LT} , Eqs. (1)-(4) become a system of four equations with four unknowns: $Q_{ev}, Q_c, T_{cho}, T_{co}$. Here, the agent provides a recommendation for the chiller leaving temperature T_{cho} .

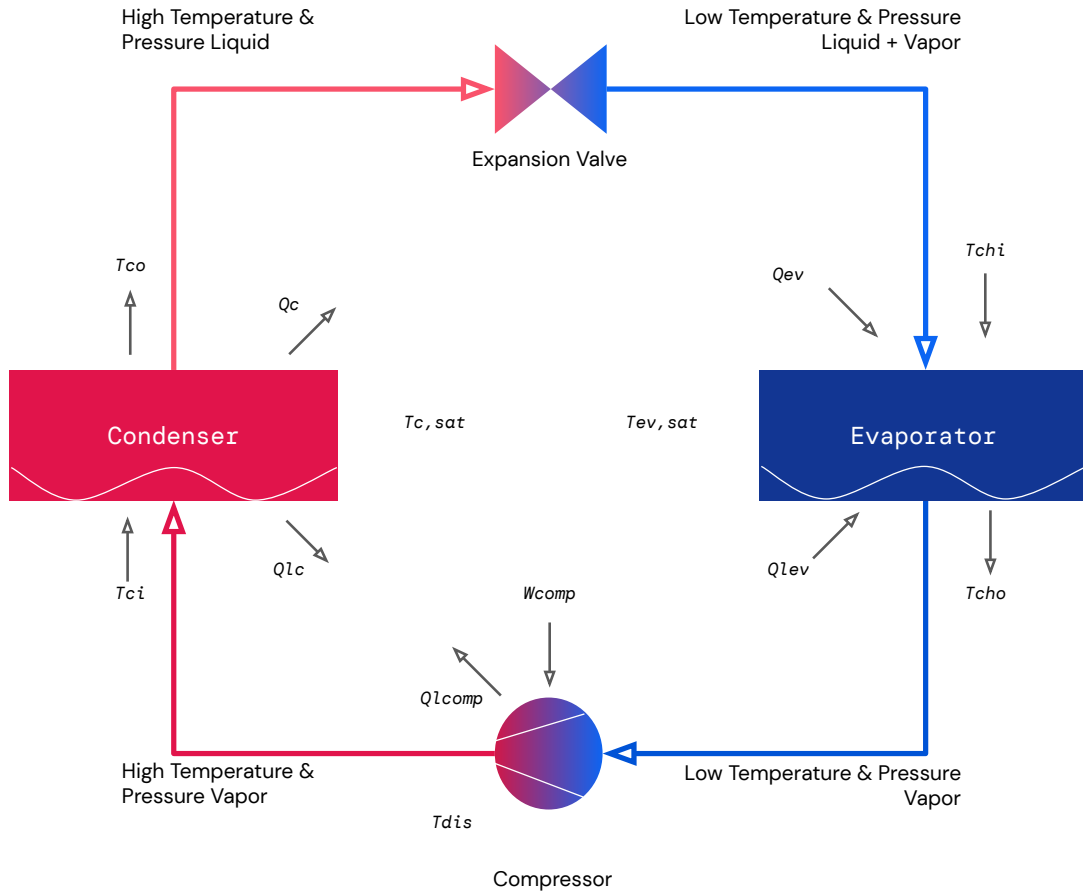


Figure 3 | Vapor-compression cycle scheme used by a chiller. T s denote temperatures and Q s denote heat. For the details see the description under Eq. 4. This diagram is adapted from [16].

Based on this, a low-level PID controller adjusts the compressor speed, hence affecting the compressor power W_{comp} parameter. This adjustment is made to minimize the error between the current sensor reading for T_{cho} with the recommendation provided. Analytically, we are now able to compute the ground truth output temperatures T_{cho}, T_{co} with auxiliary variables Q_{ev}, Q_c . Since Eq. (1) is quadratic, in order to compute Q_{ev}, Q_c one needs to select a square root branch. Matching the solution to the read data shows that one must pick the positive branch, this gives the final result:

$$T_{cho} = T_{chi} - \frac{Q_{ev}}{C_{ch}}, \quad T_{co} = T_{ci} - \frac{Q_c}{C_{cw}}, \quad (5)$$

$$Q_{ev} = \frac{-b + R}{2D}, \quad Q_c = Q_{ev} + W, \quad (6)$$

$$b = C + B + DW, \quad R = \sqrt{b^2 - D(CW - A)}. \quad (7)$$

Figure 4 shows a qualitative match between the chiller power computed via Eq. (1) and the observed data from a real facility. We see that the analytical model reproduces the observed power trends observed in the real facility. A precise match can be obtained by tuning A, B, C, D coefficients (as done in [16]).

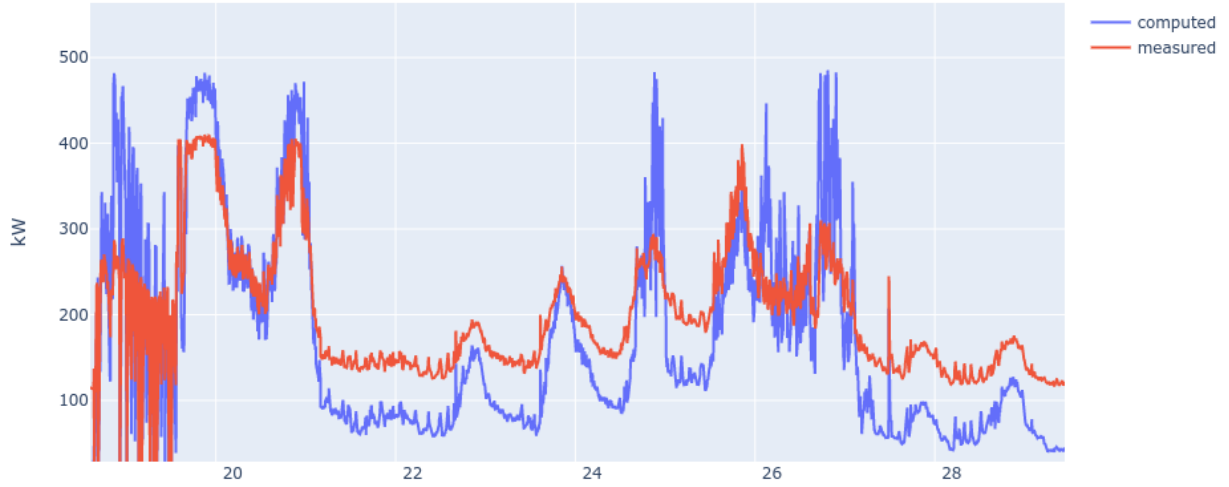


Figure 4 | Comparison of the analytical model for a chiller power Eq.(1) and the real observed data (x-axis represents days of a month). While we see a qualitative agreement, the precise match is obtained by tuning the coefficients A, B, C, D (as done in [16]).

Cooling tower Using the laws of thermodynamics, it was shown in [11] that the temperature of the water leaving the cooling tower can be computed as:

$$T_{co} = T_{ci} - (T_{ci} - T_{wb})(1 - \exp[c_8(P_{pump})^{c_9}(P_{fan})^{c_{10}}]), \quad (8)$$

where T_{ci} is the temperature of the water entering the cooling tower, T_{wb} is the wet-bulb temperature, P_{pump} is the condenser water pump frequency (speed), P_{fan} is the cooling tower fan frequency (speed). As the valve position on cooling water pipe and the resistance characteristics of the cooling water pipe unchanged, the condenser water pump flow is proportional to the water pump frequency. Similarly, the cooling tower air flow and fan power are also consistent with the law. The condenser water flow rate m_c , the condenser water pump power consumption W_{pump} , the cooling tower air flow m_a and the cooling tower fan power consumption W_{fan} are calculated [11] by:

$$m_c = c_{11}P_{pump}, \quad W_{pump} = c_{12}(P_{pump})^3, \quad (9)$$

$$m_a = c_{13}P_{fan}, \quad W_{fan} = c_{14}(P_{fan})^3. \quad (10)$$

The coefficients c_i are set by fitting the observed data (this can be done via a regression as described in [16]). Figure 5 illustrates the matching dynamics between equations for the fan/pump power and the observed data.

Multiple cooling towers Real-world cooling facilities usually have multiple cooling towers. In order to describe a real facility we need to extend Eqs.(9), (10) to multiple cooling towers. To do so, we observe that the pumps create a force to push the water, and that there are several obstructions that influence the flow. When the number of chillers and pumps are the same, we get a perfect linear relationship; when there are more pumps, the chillers' flow is weaker due to resistance. To account

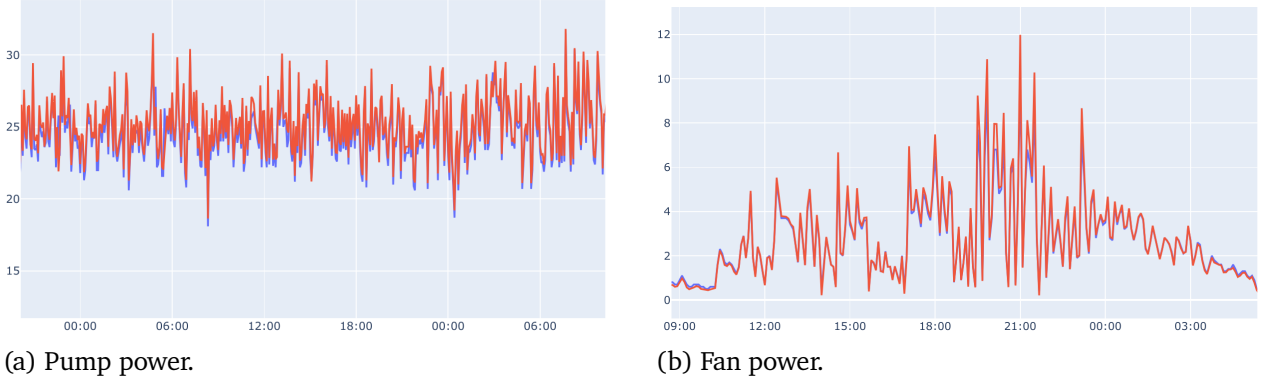


Figure 5 | Verification of equations for a pump (9) and a fan (10) power (x-axis represents times of day). Red lines represent computed values and blue lines - measured.

for this, we can introduce another term in the first equation in Eq. (9), which is proportional to the difference between the number of chillers and pumps:

$$m_c = \sum_i^N P_{pump}^{(i)} (a_1 - a_2(N_{pumps} - N_{chillers})). \quad (11)$$

Note that the number of fans might have a small effect on this as well. It turns out that this effect is negligible, as the suggested equation holds in the observed data (see Figure 6).

A further analysis shows that Eq.(8) can be easily extended for multiple pumps/fans via a simple replacement $P \rightarrow \sum_i P^{(i)}$:

$$T_{co} = T_{ci} - (T_{ci} - T_{wb}) \left(1 - \exp \left[c_8 \left(\sum_i P_{pump}^{(i)} \right)^{c_9} \left(\sum_j P_{fan}^{(j)} \right)^{c_{10}} \right] \right). \quad (12)$$

Now, we apply the above equations to the chiller plant depicted at Figure 2. We need to use inverse variations on the above equations, such that the inputs are the setpoints (plus other measured variables), and the outputs are the condenser water pump power (W_{pump}) and the fan power (W_{fan}). In our chiller plant, all pumps (and fans) are run with the same frequencies, so re-arranging (11), (10), (12) gives:

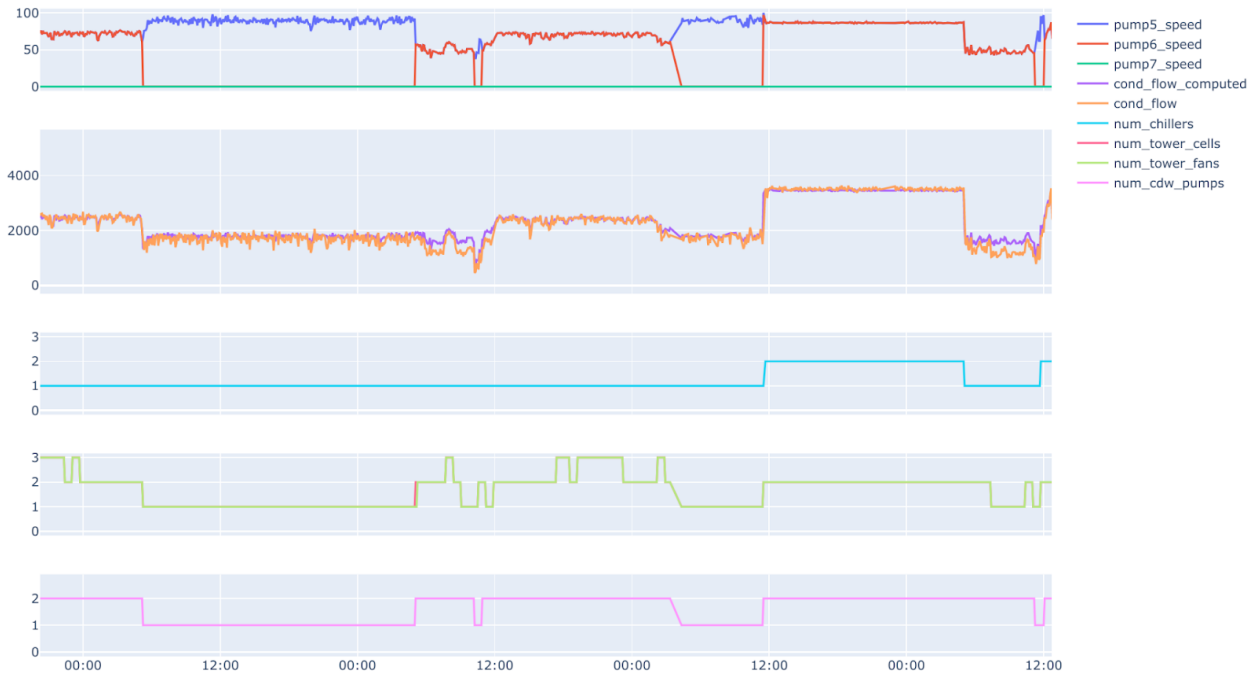
$$P_{pump}^{(i)} = P_{pump} = \frac{m_c}{c_{11} N_{pumps} (a_1 - a_2(N_{pumps} - N_{chillers}))}, \quad (13)$$

$$W_{pump}^{(i)} = c_{12} (P_{pump})^3, \quad i \in [1, \dots, N_{pumps}]. \quad (14)$$

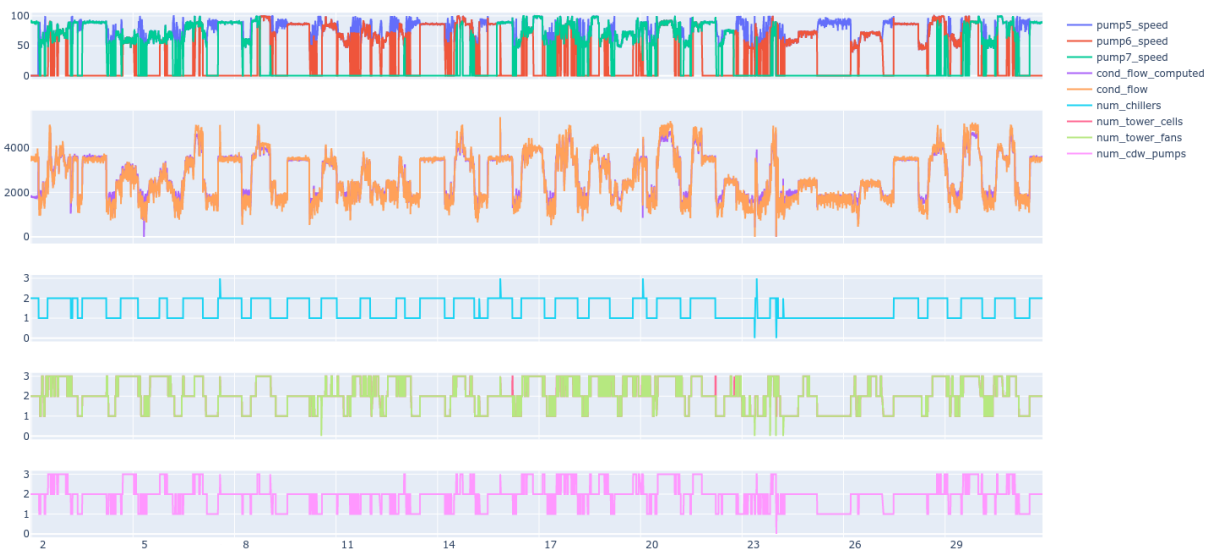
$$P_{fan}^{(j)} = P_{fan} = \frac{1}{N_{fans}} \left(\frac{1}{c_8 (N_{pumps} P_{pump})^{c_9}} \log \left[1 + \frac{T_{co} - T_{ci}}{T_{ci} - T_{wb}} \right] \right)^{1/c_{10}}, \quad (15)$$

$$W_{fan}^{(j)} = c_{14} (P_{fan})^3, \quad j \in [1, \dots, N_{fans}]. \quad (16)$$

Integrating Analytical Solutions into Multi-physics Software As described in the beginning of this section, we use a commercially available multi-physics software for modeling the fluid dynamics. This offers the flexibility to consider a wide variety of different physical processes/applications that can be solved as transient or steady state problems. In our case this software allows to define source and sinks for the physical parameters such as temperature, fluid velocity and pressure. Given the transient simulation, we extract the measured parameter values at every simulation step. Hence, we



(a) Short timescale (x-axis represents times of day).



(b) Long timescale (x-axis represents days).

Figure 6 | Verification of Eq.(11) for the condenser water flow rate under different circumstances. The second row on each figure shows a good agreement between computed vs observed flow rates for both (a) short and (b) long time scales. Figures in other rows show that the good agreement is observed for various situations including different number of chillers, fans and pumps. Here we have three pumps labeled as pump5, pump6, pump7.

leverage the simulation state variables which serve as a subset of input parameters for the analytical equations described above.

For example, in case of the Gordon-Ng chiller model, we wish to compute the temperature gradient at both the evaporator and the condenser side (see Figure 3). We consider the measured chiller inlet temperatures and mass flow rate at each of these ends. These are measured via "sensor probes" attached at the inlet of the chiller. At every simulation step, these readings are fed into the system of equations (5)-(7) and the output temperature values are computed. We assume a negligible fluid flow, pressure drop across the chiller cross section (relative to that across the facility). Next, we define a fluid flow source, which acts as the chiller outlet. The incoming water temperature is also provided by the output of the Gordon-Ng model (5)-(7). We constrain this outlet incoming differential pressure² and mass flow rate to that of the inlet measured values. This process is repeated for all chillers.

The same technique is used for the cooling tower and pump bank analytical models. The former only computes a temperature gradient similar to the chiller, and the pump bank computes the differential pressure.

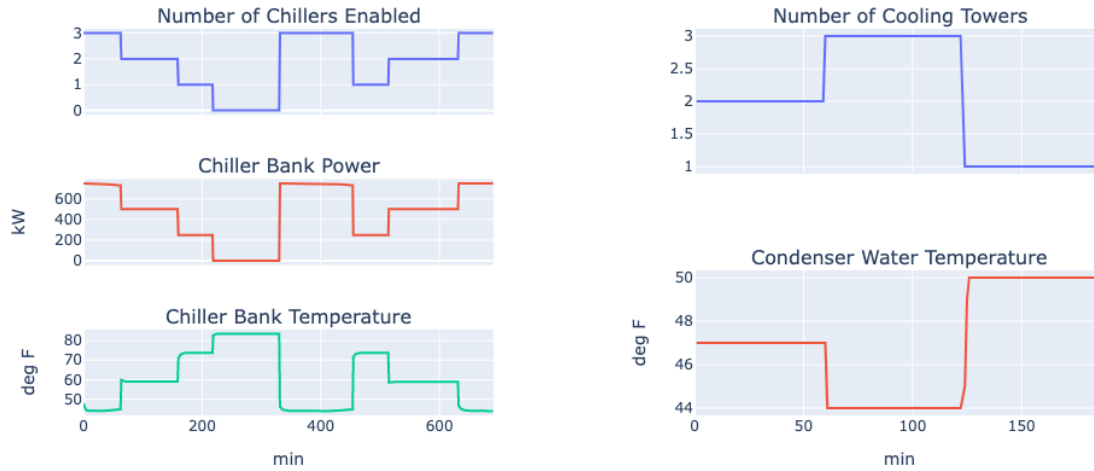
2.3. Simulation Fidelity

In the previous section, we summarized analytical solutions used as a part of our simulation and demonstrated their validity against real-world data. In this section we provide some additional fidelity checks for the entire simulation, which combines the analytical solutions with simulation software libraries as described above.

We start with simple demonstrations in Figure 7. First, keeping all setpoints fixed, we vary the number of chillers. As expected, turning on more chillers decreases the system's temperature and turning off chillers have the opposite effect (see Figure 7a). Second, we vary the number of cooling towers. Again, as expected, turning on more cooling towers decreases the system's temperature and other way around - turning off cooling towers increases the temperature (see Figure 7b). As a slightly different example, we fix the chiller leaving temperature setpoint and increase the dry bulb temperature, which represents the external weather conditions. As expected, we observe (Figure 7c) an increase in the compressor power required to maintain the chiller temperature. After leaving the air handling unit (AHU), the water gets progressively warmer due to the greater heat generated from the building (which is modeled as the increase in the dry bulb temperature). We also see the intermediate transitions in the temperature as the PID controllers try to control the chiller power. After a rapid transition due to the increase in dry bulb temperature, the PIDs react by reducing the power.

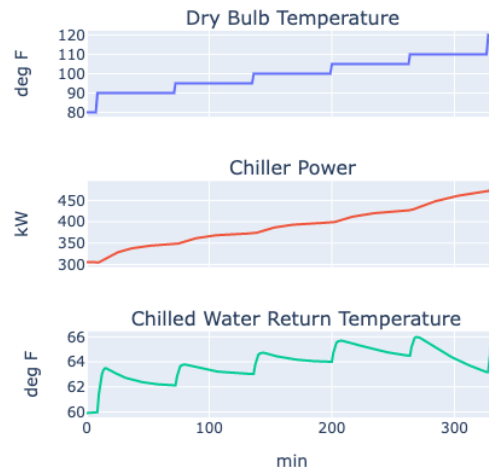
Next, we demonstrate that our simulation exhibits a more complex "emergent" behavior. Since chillers are usually the most energy-intensive components of any cooling facility, it is important to efficiently control how many chillers are used at any given time. The domain experts know that depending on external conditions, there are regimes when it is more energy-efficient to use two chillers even though a single chiller can achieve the desired temperature. To show that our model encodes this information, we plot the total power used by all chillers as a function of dry bulb temperature. For each value of the dry bulb temperature we show the total power used by different number of chillers (see Figure 8a). This needs to be compared to the real world data. To do so, we display the total power used by all chillers as a function of load (in our simulated environment dry-bulb temperature is a proxy for the load). For each value of the load we show the total power used by different number of chillers. For low values, one chiller always consumes the lowest amount of energy. However, for

²The differential pressure is defined as the difference in pressure between two points in the water pipes. In the case of the chilled water system, the differential pressure at any point is measured relative to the pressure at the chilled water pump inlet.



(a) Changing the number of chillers.

(b) Changing the number of cooling towers.



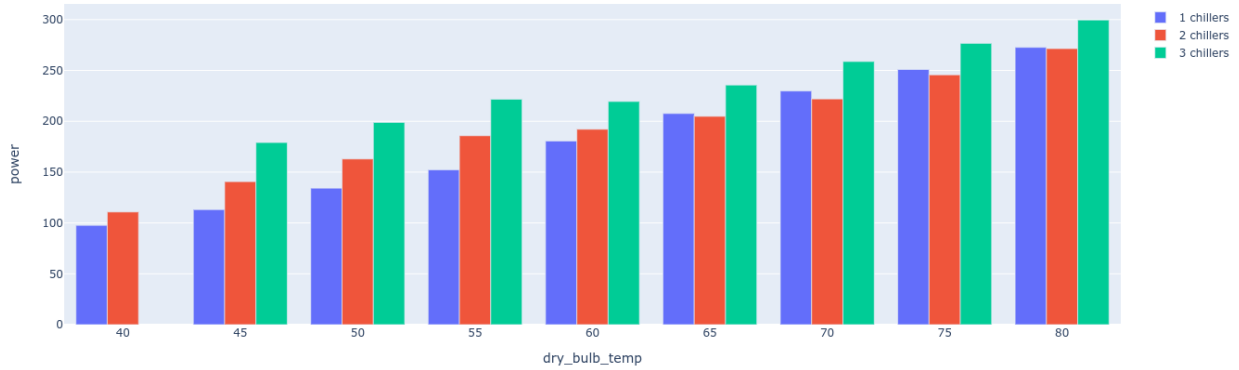
(c) Increasing the dry bulb temperature.

Figure 7 | High level simulation fidelity check. Increasing the number of chillers (a) or (b) number of cooling towers decreases the overall temperature in the system. Similarly, in (c) an increase in the external temperature, increases the chiller power consumption.

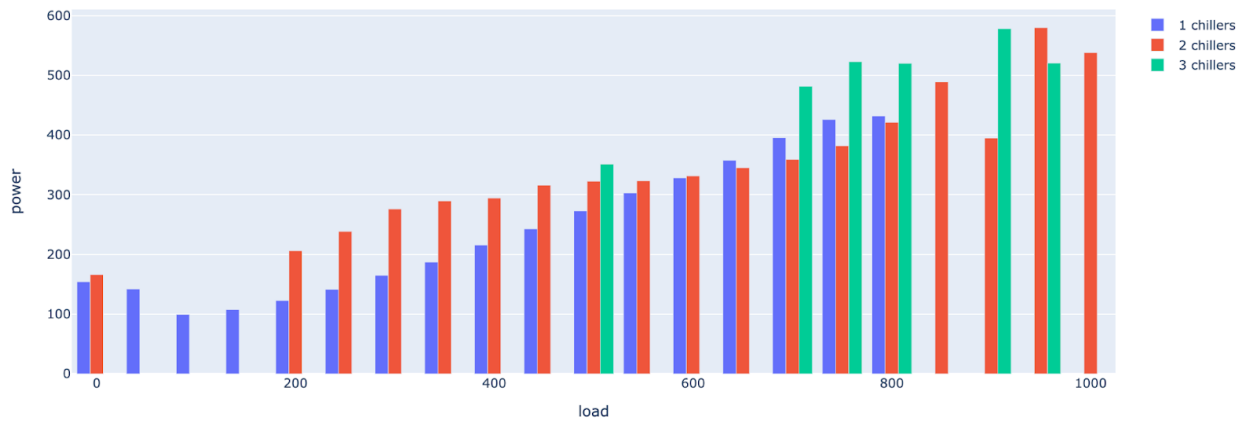
higher values two chillers are more energy efficient. We observe the quantitative match between the simulated and observed transitions from real world data.

3. Reinforcement Learning Applications

To demonstrate how our industrial cooling system model (Section 2) can be used for reinforcement learning applications, in this section we introduce the Industrial Task Suite, define several tasks for the model, and use these tasks to evaluate the performance of different RL algorithms.



(a) Simulated data.



(b) Real data.

Figure 8 | Total power consumed by all chillers as a function of dry-bulb temperature (load). We see that for low dry bulb temperatures (load) it is always more energy-efficient to use one chiller. Two chillers become more efficient for high values of the dry-bulb temperature (load).

3.1. Industrial Task Suite

We begin with the Industrial Task Suite, a flexible framework for defining industrial control problems within a reinforcement learning context. It allows to create environments and tasks to train and evaluate artificial controllers safely and efficiently, subject to various real world conditions, such as sensor imperfections and white noise. ITS is in-line with the design of the DeepMind Control Suite [36] and Real-World Reinforcement Learning (RWRL) Challenge Framework [15], while providing more granular configurability of environments. Balancing ease-of-use and customization, the task suite only requires a simulation (model) and a task to define a RL problem (Figure 9), and yet offers a highly parameterized facility configuration, which provides industrial equipment components with customizable capacities, amounts and connection topology. The task suite also supports specific scenarios such as sensor noise/drift, weather variations, and varying initial conditions to mimic specific real-world operating regimes. A diversity of such "frozen" scenarios could serve as a test bed for evaluating performance and benchmarking against existing baselines.

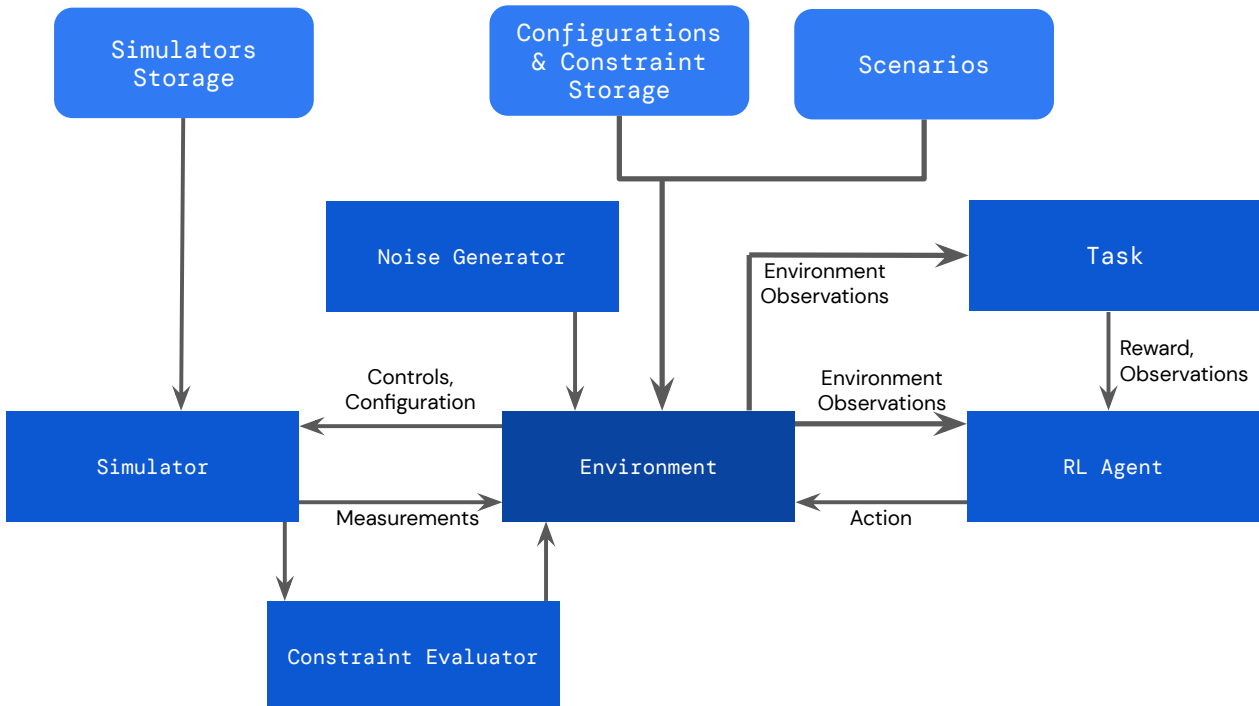


Figure 9 | The Industrial Task Suite design diagram. The `Environment` class orchestrates the main components: `simulator`, `noise generator`, `task`, `constraint evaluator` and `agent`. It takes a configuration and uses it to initialize a simulation loaded from the simulator database. It then starts relaying the traffic between the agent and the simulator.

The core `Environment` class encapsulates and orchestrates the following components: `simulator`, `noise generator`, `task`, `constraint evaluator` and `agent` (see Figure 9). It takes a configuration from the database and uses it to initialize a simulation. Then `Environment` applies one or several implemented scenarios and defines the constraints. It uses a pre-defined `task` to compute rewards and expand the observations space with additional information. It then starts relaying the traffic between the agent and the simulation. While doing so, it injects noise into the exchanged data, evaluates the constraints and calculates the rewards.

`Environment` converts the inbound actions sent by an agent into simulation control signals, and subsequently convert the outbound simulation measurements into observations. Given a broad range of possible control/measurement specs, the converters pad the values to a defined maximum range and append masks to the observation to inform the agent about the differences in the configuration. In order to provide access to all of the available information, the facility configuration and the spec definition is also added to the observation dictionary. Should that information be obsolete for a particular agent architecture, it can be filtered out in an environment wrapper.

`Noise` is added to the control signal and to the observation respectively. The noise simulates sensor/pipeline imperfections, and in effect diversifies the distribution of simulated states (control noise) and observations (observation noise). At each episode step, in addition to sending the control signal, `Environment` also changes the values of the selected configuration parameters according to pre-defined `scenarios`. This allows simulating the changing environment conditions and other environmental instabilities.

A more detailed overview of ITS's main components along with some implementation details are given in Appendix A.

Action	Unit	Type	Default	Minimum	Maximum
# Chillers Enabled	-	Integer	1	0	3
# Chilled Water Pumps	-	Integer	1	1	3
# Condenser Water Pumps	-	Integer	1	1	3
Chiller Leaving Temperature	deg F	Continuous	48	40	75
Cooling Tower Return Water Temperature	deg F	Continuous	55	32	90
Condenser Water Pump Flow rate	kg/s	Continuous	50	10	200
Distributional Differential Pressure	psi	Continuous	15	0.1	50
# Free cooling Heat Exchangers	-	Integer	1	1	3

Table 1 | Action space used in our experiments.

3.2. Tasks

The goal of an AI-powered system that operates a cooling facility is to minimize the energy consumption while meeting a set of constraints. For industrial cooling systems these constraints are defined to ensure that buildings are comfortable for the people inside and to prevent the equipment breakage. To efficiently train RL agents within the ITS framework, we consider a curriculum learning based approach [9] (for a recent review see [34]). Namely, we define various tasks categorized by their perceived complexity and teach agents to solve them sequentially. Eventually, we will have an agent that knows how to solve all the tasks and operate the cooling facility.

We start with action (Table 1) and observation (Table 2) space defined for our simulator (Section 2). All values are selected based on a typical industrial cooling facility configuration.

Observation	Type	Unit
Building load	Continuous	kW
Dry bulb temperature	Continuous	deg F
Wet bulb temperature	Continuous	deg F
Relative humidity	Continuous	-
Condenser leaving temperature (per chiller)	Continuous	deg F
Chilled water flow rate (per chiller)	Continuous	kg/s
Compressor power (per chiller)	Continuous	kW
Cooling tower fan power	Continuous	kW
Condenser water pump bank power	Continuous	kW
Chilled water pump bank power	Continuous	kW
Chiller bank leaving temperature	Continuous	deg F
Chilled water supply temperature	Continuous	deg F
Chilled water return temperature	Continuous	deg F
# of chillers enabled	Integer	-

Table 2 | Observation space used in our experiments.

To mimic the industrial setting, the constraints are split into soft and hard. A hard constraint violation terminates the episode (the agent gets kicked out of the environment), which incentivizes the agent to respect the constraint. Soft constraints can be added to the reward function via additional terms (for more see Section 3.3). Additionally, any constraint violation is communicated to the agent as an observation. For more about constraints see Section A.4.

Next, we list several tasks sorted by difficulty and provide (if known) corresponding baseline and the optimal policies.

Easy

Unconstrained number of chillers control *Controls*: number of chillers (1D integer). *Baseline policy*: use 0 chillers. *Optimal policy*: use 0 chillers. This is a very simple task, where we do not impose any constraints and not worry about any temperatures in the system. Ultimately, controlling the number of chillers is the most important aspect of a cooling facility control, because chillers are the most power-consuming components.

Constrained number of chillers control *Controls*: number of chillers (1D integer). *Hard constraint*: use only a subset of available chillers, for example, if there are 3 available chillers, the agent is allowed to use only 1 or 2 chillers. *Baseline policy*: use 1 chiller. *Optimal policy*: use 1 chiller. This is a slightly more complicated chiller control task, where we still do not worry about the temperatures, but impose the constraint on the number of chillers. Via this task we explore whether the agent can learn to satisfy hard constraints.

Chiller temperature control *Controls*: chiller temperature (1D float). *Baseline policy*: use the highest possible chiller temperature. *Optimal policy*: use the highest possible chiller temperature. In a typical cooling facility, along with the number of chillers, one can control individual chiller temperatures. With this task we investigate whether the agent can learn to effectively control them.

Medium

Constrained number of chillers control with an additional constraint on the chilled water supply temperature *Controls*: number of chillers (1D integer). *Hard constraint*: use only a subset of available chillers and constraint on the range of chilled water supply temperature. *Scenario*: Randomized dry-bulb temperature. *Baseline policy*: use 1 chiller. *Optimal policy*: depending on the external conditions use 1 or 2 chillers. This task is closer to real facility requirements; the agent controls the number of chillers while keeping the chilled water supply temperature within a given range, which directly translates to the overall temperature in a building and its occupants' comfort.

Number of chillers and condenser temperature control with an additional constraint on the chilled water supply temperature *Controls*: number of chillers (1D integer) and condenser temperature (1D float). *Hard constraint*: constraint on the range of chilled water supply temperature. In this task, in addition to the number of chiller control, the agent controls the condenser temperature while keeping the chilled water supply temperature within a given range.

Hard

Full cooling system control *Controls*: All actions defined in Table 1. *Hard constraint*: constraint on the range of chilled water supply temperature. In this task the agent controls all available cooling facility setpoints while keeping the chilled water supply temperature within a given range.

Other tasks

For a fixed simulator the new tasks can be constructed by using one or a combination of several possible ways:

- Selecting a task objective (for example, minimize the power consumption).
- Adding a scenario (for example, changing weather).

- Selecting a subset of controls (for example, only control the number of chillers).
- Adding noise to controls.
- Adding noise to measurements.
- Imposing constraints.

3.3. Reward Function

As discussed in Section 3.2, we split constraints into soft and hard, where a hard constraint violation terminates the episode, and soft constraints are added to a reward function via additional terms. Moreover, any constraint violation is communicated to the agent as an observation. The base reward function (without soft constraints) should satisfy the following requirements:

1. Inverse relationship between power and reward (more power - less reward).
2. Maximum reward = 1 (when the power is 0, which is the best case scenario, the reward is 1).
3. Reward function is sensitive to a change in the relevant range of power (this depends on the cooling system configuration).

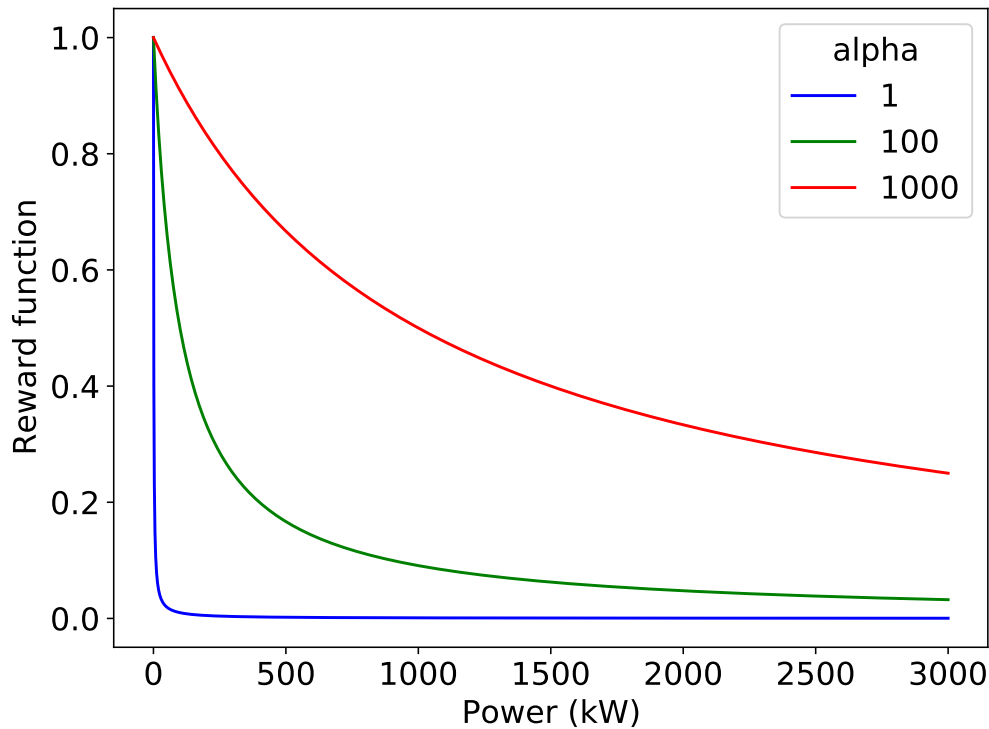


Figure 10 | Base reward function for power optimization tasks - Eq. (17). The normalization constant, α , allows to make the reward function sensitive to the power change in the relevant range of values. In this example, when $\alpha = 1$ the reward function has nearly the same value for the entire 10-3000 kWatt range. $\alpha = 1000$ provides a good gradual reward change from 10 to 3000 kWatts.

The following simple function satisfies all the requirements:

$$r = \frac{1}{W/\alpha + 1}. \quad (17)$$

Here W is the power consumed by the system and α is a normalization constant. 1 in the denominator ensures that $r(0) = 1$ and the normalization constant (α) makes the function sensitive to the relevant range of power. For example, for industrial chillers $\alpha \sim 1000$ in the SI units (kWatt).

3.4. Experiments and Results

We now investigate whether the common deep RL algorithms can be used for the industrial cooling facility control by benchmarking these algorithms on some of the tasks defined in Section 3.2. We consider DMPO [3, 7], DDPG [28], D4PG [8], and use their ACME implementations [22]. For some of the tasks we know the optimal policy and will see if the RL agents are able to learn it.

For all agents we employ the continuous action space normalized to $[-1, 1]$. If controls are integer-valued we quantize the agent’s continuous actions³. Each agent was run 3 times per task using different seeds. For all tasks we use episodes of length 10. Figure 11 shows performance on individual tasks, where the lines denote the mean return and the shaded regions denote standard deviation across seeds. For easy tasks we use 10 actors per agent and for the medium task - 100. We used the same hyperparameters across all tasks (i.e. so that nothing is tuned per-task). Due to a slow simulator, we had to use mini-batches of size 4 across all tasks, and frequently update the actor networks - every 10 actor steps.

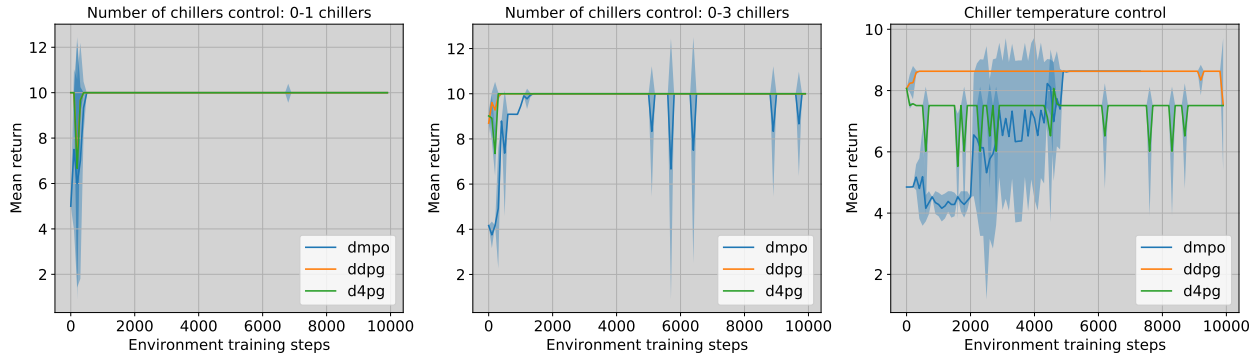
The summary of results is presented on Figure 11. For our experiments we consider tasks for controlling the number of chillers and the chiller temperature. As motivated in Section 3.2, these are the most important setpoints for an effective cooling facility control. For the number of chillers control, we start with a very simple binary configuration: the agent can select 0 or 1 chiller. All agents learn this trivial task very fast (in ~ 100 training steps). Next, we use the configuration with 4 states: the agent can choose between 0, 1, 2, and 3 chillers. And again all agents learned this task easily, although DMPO took a bit longer while also experiencing a few spikes in the mean return across different seeds. For the chiller temperature control, DDPG converges to the optimal policy very fast, while D4PG converges to a sub-optimal policy across all seeds. DMPO does learn the optimal policy, but again it converges slower than DDPG. Finally, we consider a medium difficulty task: the agent controls the number of chillers (0, 1, 2, 3 chillers are available), but if it selects 0 or 3 chillers the episode terminates; there is also additional constraint on the chiller water supply temperature, which directly maps to the overall building temperature. In this case DMPO is the only agent to learn the optimal policy. Overall, we see that DMPO performs the best, as it learns the optimal policies for all four tasks. Next, we provide more details on the architectures for each agent.

DMPO Both policy and critic networks are LayerNorm MLPs - they are MLPs with ELU non-linearities preceded by a linear layer followed by a LayerNorm and tanh activation: $Linear \rightarrow LayerNorm \rightarrow tanh \rightarrow Linear \rightarrow ELU \rightarrow Linear \rightarrow ELU \rightarrow \dots$. The policy network had three layers of [256, 256, 256] units respectively. Actions are sampled from a multivariate Gaussian with diagonal covariance, parameterized by initial and minimum scale parameters for which we use the default values of 0.3 and 10^{-6} respectively. The critic network had three layers of [512, 512, 256] units, the output of the last layer is concatenated with the actions and passed into the discrete valued head that returns the categorical distribution, using 51 categories spaced evenly across $[-15, 15]$.

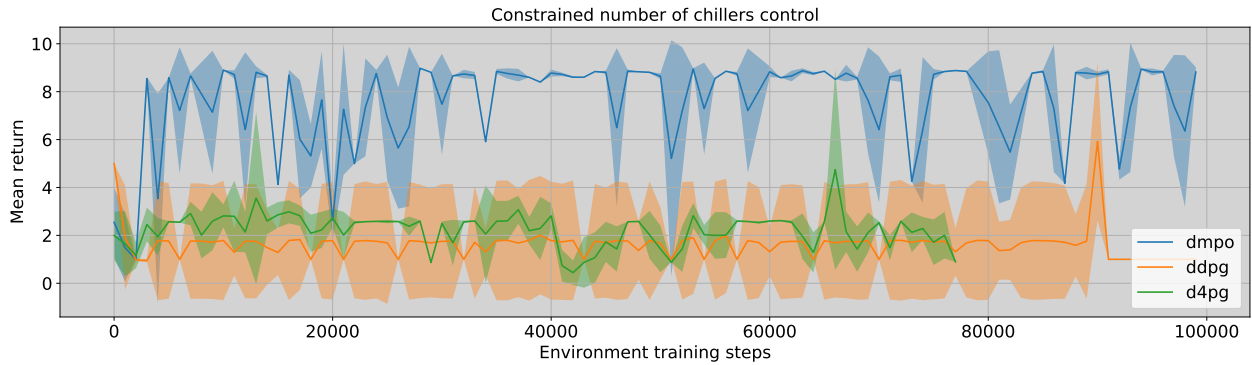
DDPG Just like in case of DMPO both policy and critic networks are LayerNorm MLPs where we use the same hyperparameters. The policy network is the LayerNorm MLP with [256, 256, 256] units. The critic network concatenates observations and actions and passes them into the LayerNorm MLP with [512, 512, 256] units, which go into another Linear Layer with output dimension 1.

D4PG For D4PG we use the critic network from DDPG and the policy networks from DMPO with the same hyperparameters.

³This is done for simplicity since the agents we consider are designed for continuous actions.



(a) Easy tasks.



(b) Medium task.

Figure 11 | Comparison of DMPO, DDPG and D4PG on the tasks defined for our simulated cooling system environment. We consider three easy and one medium tasks defined in Section 3.2. Easy tasks include: unconstrained chiller control (a binary 0-1 chillers and non-binary 0-3 chillers) and a chiller temperature control. For the medium task we use the constrained number of chiller with an additional constraint on the chilled water temperature. Note that for each task we run an experiment with three seeds and report the mean return and uncertainty (shaded area). Interestingly, DMPO is the only agent that learned the optimal policy for all the tasks (for optimal policies and max returns see Section 3.2).

4. Limitations

Some limitations of our model and the Industrial Task Suite include:

- *Simulation Speed*: The simulation software solves complex ordinary differential equations at every step. Even with our hybrid analytical model, this results in a magnitude of ~ 10 seconds/step with each step simulating a real world 5 minute time horizon. With the current setup, this doesn't match the high frequency iterations of existing reinforcement learning environments. A next step would involve optimizing the environment setup and the solver for faster simulated transitions.
- *Simulation Fidelity* The simulator fidelity checks described in this paper are not exhaustive; more work is required to ensure its accuracy.
- *Sim2Real Validation*: We have designed and implemented the Industrial Task Suite to enable domain randomization, a technique that randomizes the simulator parameters to expose the agent to a diverse set of environments in the training phase. Additionally, it provides access to a wide diversity of real world scenarios. However, it remains a future work to develop a Sim2real adapter to integrate this with a real world facility.

The modular Industrial Task Suite, as well as the hybrid simulation model design, have been described in detail. While this should be descriptive to provide a high level understanding of the contribution, releasing the codebase remains out of scope for this work.

5. Conclusions

Designing and evaluating accurate whole-facility industrial cooling models is a challenging optimization problem. In this paper, we presented one possible approach by combining analytical solutions with a multi-physics simulation software. We showed that it empirically matches key properties of real-world facility behavior.

We extended and demonstrated the usability of this model by providing the design for an Industrial Task Suite, which allows custom RL problem configurations using our model or any other physical control simulator. We benchmarked RL agents using this task suite and identified DMPO to be a well-performing candidate for the problem of cooling system control, as it found the optimal policies for all four given tasks. Providing this model and framework, we hope to make applying RL to the real-world problem of optimizing industrial controls more accessible.

Appendix

A. Industrial Task Suite Components

In this section we will briefly describe all components of the task suite defined in Section 3.1 and provide some implementation details.

A.1. Environment

`Environment` extends `dm_env.Environment`, an abstract base class for RL environments defined in The DeepMind RL Environment API [31]. Its main job is to comprise and orchestrate all components (see Figure 9).

```
class Environment(dm_env.Environment):
    def __init__(self,
                 simulator: SimulatorInterface,
                 task: TaskInterface,
                 evaluator: Evaluator,
                 initial_conditions: Mapping[str, Any],
                 initial_conditions_noise: Mapping[str, float],
                 controls: Collection[str],
                 controls_noise: Mapping[str, float],
                 measurements: Collection[str],
                 measurements_noise: Mapping[str, float]
                 ...)
        self._simulator = simulator
        self._task = task
        self._evaluator = evaluator
        ...
        self._ic = initial_conditions
        self._ic_noise = initial_conditions_noise
        ...
        self._controls_noise = controls_noise
        ...

    @property
    def action_spec(self):

    @property
    def observation_spec(self):

    def reset(self):
        # Add noise to initial conditions.
        noisy_cfg = {}
        for ic_id, ic_value in self._ic.items():
            noisy_cfg[ic_id] = ic_value + self._ic_noise[ic_id]

        # Reset the simulator with the new noisy initial conditions
        timestep = self._simulator.reset(noisy_cfg)

        # Add noise to measurements and evaluate constraints
        core_obs, _ = process_timestep(timestep, self._evaluator)

        # Reset task.
        task_obs = self._task.reset(noisy_cfg, core_obs)

        observation = dict(**core_obs, **task_obs)
        return dm_env.restart(observation)

    def step(self, action):
        # Add noise to controls (actions)
```

```
for action_id in action:
    action[action_id] += self._controls_noise[action_id]

timestep = self._simulator.step(action)

# Add noise to measurements and evaluate constraints
core_obs, hard_constraint_violation = process_timestep(timestep, self._evaluator)

# Compute reward and extend observation
reward, task_obs = self._task.calculate_reward_and_observations(
    core_obs)

observation = dict(**core_obs, **task_obs)
if timestep.is_last or hard_constraint_violation:
    return dm_env.termination(reward, observation)
else:
    return dm_env.transition(reward, observation)
```

A.2. Tasks

Tasks are designed to exercise orthogonal areas of competence, but at the same time work with any configuration sampled from the defined distribution. In addition to that, the shared component framework allows testing out certain policies on the entire range of tasks. From the implementation point of view tasks define and compute rewards as well as provide additional observations to the agent.

```
class TaskInterface:

    @property
    def observation_spec(self):

    def reset(self, configuration):

    def calculate_reward_and_observations(observation):
```

A.3. Simulator

A simulator is the ground-truth model of the system dynamics. It is configured at the beginning of each new episode. That is the moment when a new configuration will be sampled. This means that at each new episode, a new simulation might be selected as well. Once the simulator is configured it starts taking controls from the agent at every agent step and returns the results in the form of measurements, which are a subset of the simulation state.

```
class SimulatorInterface:

    @property
    def measurement_spec(self):

    def reset(self, configuration):

    def step(self, controls):
```

A.4. Constraints

Constraints are defined in a configuration file. In the industrial setting the agent gets kicked out of the system, when it violates some constraints, to mimic this we divide constraints into hard and soft. Violation of a hard constraint automatically ends an episode (equivalent to the agent being kicked out

of the system). Violation of any of these constraints is communicated to the agent as an observation. Constraints are evaluated on every step - after receiving an agent's action, and subsequently after receiving an updated simulation measurements. The constraint evaluator is used in both cases to validate them.

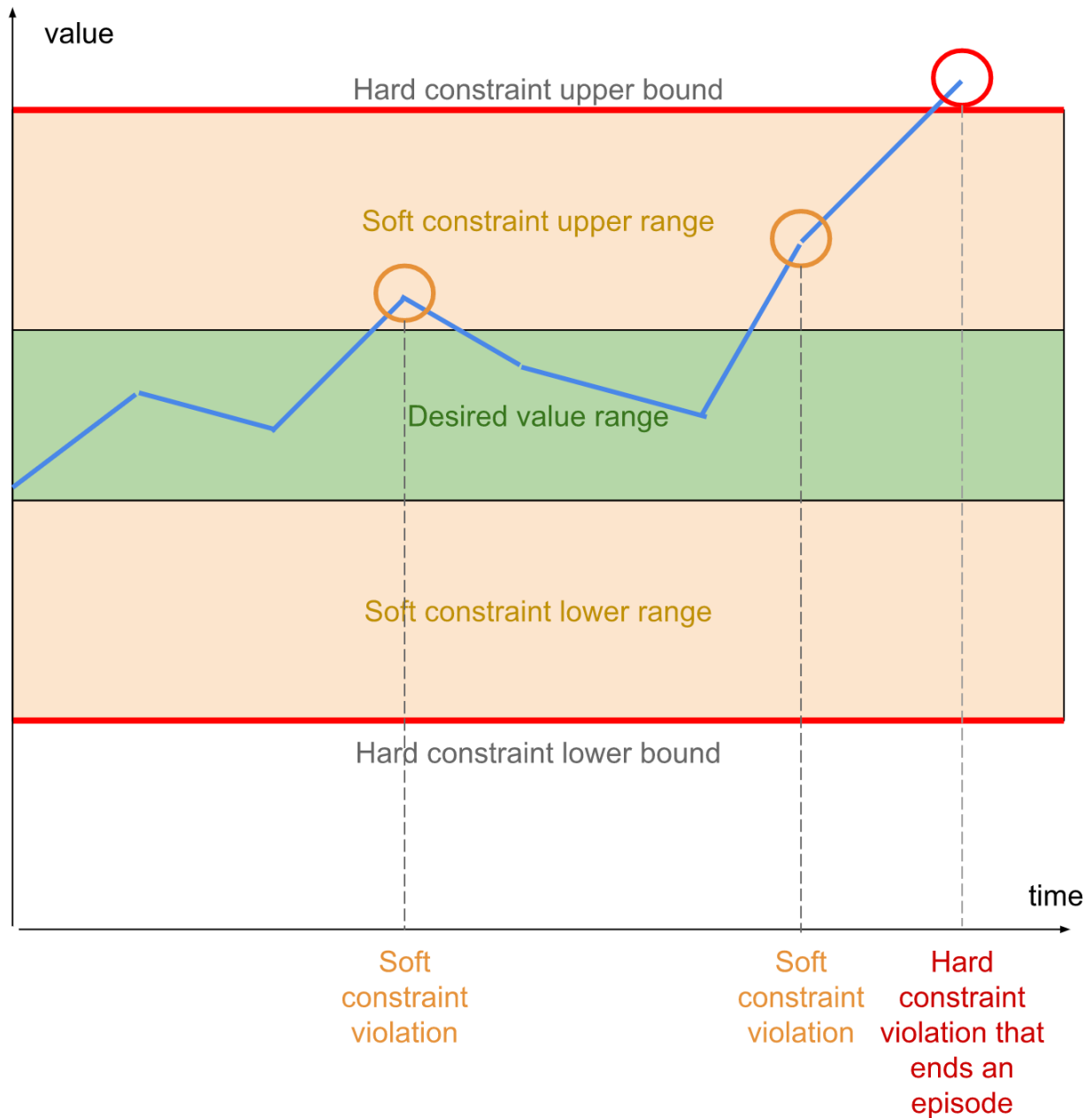


Figure 12 | Evaluation of the constraint ranges for a single value.

Hard constraints can be expressed by a single range of values. Soft constraints define ranges bounded by the hard constraint upper and lower limits. This can be expressed with a custom structure that defines four values for each of the limits.

```
class Constraint:
    simulation_parameter_name: str
    hard_upper: float
```



```
soft_upper: float
soft_lower: float
hard_lower: float
```

The values should meet the following criteria $\text{hard_lower} \leq \text{soft_lower} < \text{soft_upper} \leq \text{hard_upper}$.

A.5. Scenarios

Scenarios add another configuration dimension to the environment. Each scenario describes a trajectory that modifies a set of simulation configuration parameters. Along with noise, scenarios make environment more realistic. Below we list a set of scenarios each representing a challenge we observed in the real world industrial systems.

- **Frozen sensors:** The scenario freezes the values of selected sensors for a random amount of time. A dedicated implementation of the measurement noise handles this. Its purpose is to test an agent’s resilience to missing information.
- **Sensor drift:** The scenario introduces a temporally correlated noise into the selected measurement components. The components are selected at random at the beginning of each episode. Its purpose is to test an agent’s resilience to partially false information.
- **Frozen controls:** The scenario freezes the values of selected controls for a random amount of time. A dedicated implementation of the control noise handles this. Its purpose is to test an agent’s ability to detect when a selected policy fails and adapt by switching to an alternative.
- **Simulation dynamics non-stationarity:** The scenario uses a set of configuration trajectories to modify the selected simulation configuration parameters over the course of an episode. Configuration trajectories produce changes to selected parameters, which the task adds to their baseline values and subsequently passes to the simulation. Control tensor is used for that purpose. Absolute configuration values are used so that limits can be observed. The limits are stored in the configuration definition. Its purpose is to test an agent’s resilience to ever changing environmental conditions, for example, weather change and other variables outside the domain of agent’s control.

B. Other Industrial Task Suite Applications

The modularity of the industrial task suite and the tools developed around the cooling system simulation model allow the easy implementation of other control problems of interest, which might have very different physics and task definitions.

B.1. Brushless DC motor

Direct control electrical machines is a long standing research problem for industrial control systems, and using reinforcement learning based control approaches offers potential to improve on the state-of-the-art performance of existing controllers.

In order to explore research into this area, we have implemented a simulation model for a Brushless DC (BLDC) electrical motor using COMSOL. The simulation model is a 2D axial cross-section of a 3-phase electrical motor, with a magnetized rotary core (see Figure 13). The agent observes the angular position and velocity of the rotor, and controls the currents being applied to each of the three phase coils. The simulation also allows us to visualize (Figure 13-2) the magnetic field intensity of the simulated motor.

We have successfully trained a DMPO agent [7, 3] to control the motor in a generic trajectory tracking task. A random target position trajectory is created and sent to the agent; and a reward is calculated based on the difference between the actual and target positions, with reward = 1 when they are

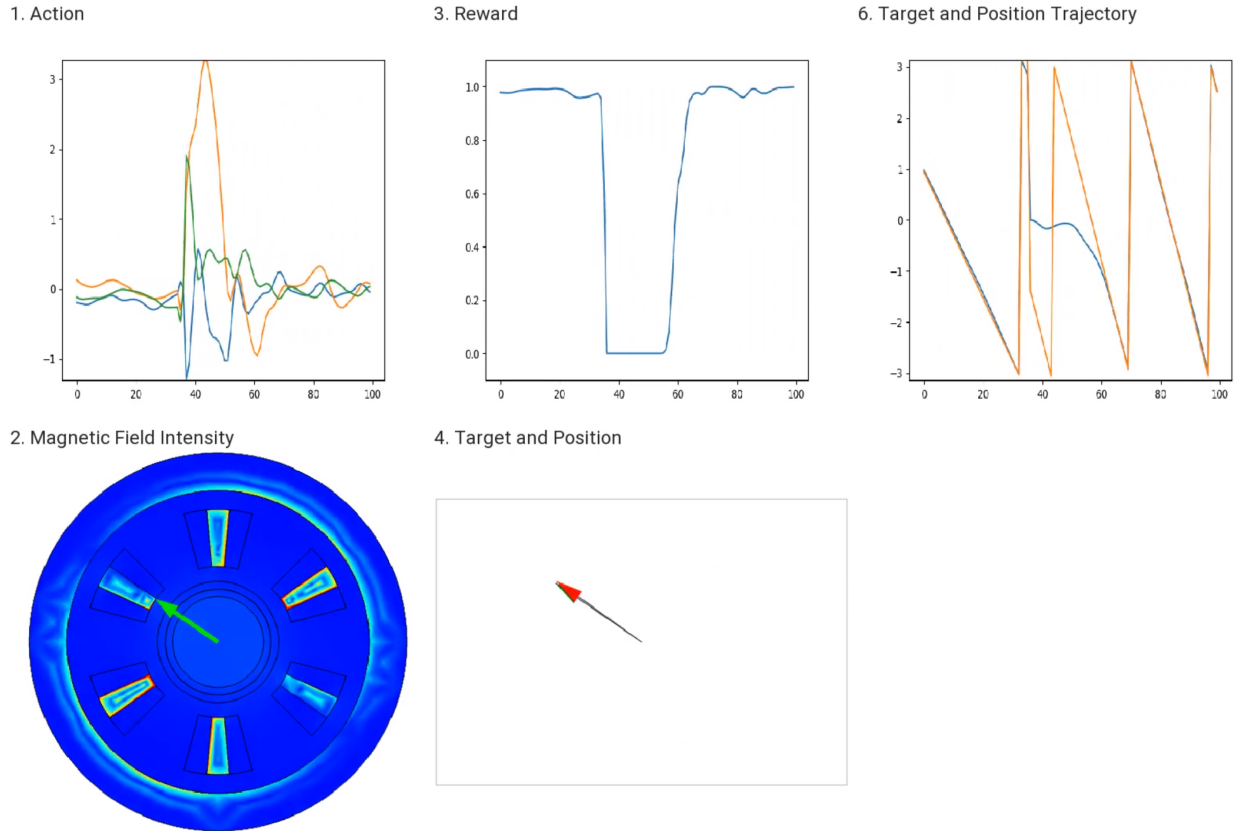


Figure 13 | BLDC motor simulation environment captured as stills from video [5]. The agent sets actions in the form of three phase currents (top left), to control the motor. (Bottom Center) Target position is shown with a red arrow and the current position is shown with a green arrow.

equal. The agent also uses a secondary objective to reduce the size of actions ("phase currents"), to minimize power.

B.2. Airfoil

Another example domain with complex physics is fluid flow. Flight control systems aim to achieve lift and stability while countering non-linear and time-varying physics [24]. This domain provides a challenging test domain for our agents and our methods for providing and soft/hard constraints to achieve stability.

We have implemented an airfoil under flow to control the altitude. The agent observes the current altitude, a target altitude and current pitch of the airfoil in addition to the lift force generated, and controls the rate of change of the pitch. We have implemented a DMPO agent to learn a control policy that achieves a target altitude. We have successfully demonstrated this policy in the following video [4].

References

- [1] Britannica, t. editors of encyclopaedia (2016, february 16). cooling system. encyclopedia britannica. <https://www.britannica.com/technology/cooling-system>.
- [2] Deepmind ai reduces energy used for cooling google data centers by 40 <https://blog.google/outreach-initiatives/environment/deepmind-ai-reduces-energy-used-for/>. Accessed: 2022-07-26.

- [3] Distributional maximum a posteriori policy optimization (dmpo). <https://github.com/deepmind/acme/tree/master/acme/agents/tf/dmpo>. Accessed: 2022-07-11.
- [4] Dmpo agent learns to control a airfoil under fluid flow. <https://youtu.be/fGRDnwYYJnw>. Accessed: 2022-07-12.
- [5] Dmpo agent learns to control a bldc motor to achieve "constant speed" task. <https://youtu.be/dR2cT8cRTlw>. Accessed: 2022-07-12.
- [6] Industrial sector energy consumption. <https://www.eia.gov/outlooks/ieo/pdf/industrial.pdf>.
- [7] A. Abdolmaleki, J. T. Springenberg, Y. Tassa, R. Munos, N. Heess, and M. Riedmiller. Maximum a posteriori policy optimisation. *arXiv preprint arXiv:1806.06920*, 2018.
- [8] G. Barth-Maroon, M. W. Hoffman, D. Budden, W. Dabney, D. Horgan, D. Tb, A. Muldal, N. Heess, and T. Lillicrap. Distributed distributional deterministic policy gradients. *arXiv preprint arXiv:1804.08617*, 2018.
- [9] Y. Bengio, J. Louradour, R. Collobert, and J. Weston. Curriculum learning. In *Proceedings of the 26th annual international conference on machine learning*, pages 41–48, 2009.
- [10] G. Brockman, V. Cheung, L. Pettersson, J. Schneider, J. Schulman, J. Tang, and W. Zaremba. Openai gym. *arXiv preprint arXiv:1606.01540*, 2016.
- [11] Y. Cao, L. Huang, Z. Cui, and J. Liu. The optimal operation of cooling tower systems with variable-frequency control. In *IOP Conference Series: Earth and Environmental Science*, volume 113, page 012085. IOP Publishing, 2018.
- [12] B. Chen, Z. Cai, and M. Bergés. Gnu-rl: A precocial reinforcement learning solution for building hvac control using a differentiable mpc policy. In *Proceedings of the 6th ACM international conference on systems for energy-efficient buildings, cities, and transportation*, pages 316–325, 2019.
- [13] Y. Chen, Y. Shi, and B. Zhang. Optimal control via neural networks: A convex approach. *arXiv preprint arXiv:1805.11835*, 2018.
- [14] D. B. Crawley, L. K. Lawrie, F. C. Winkelmann, W. F. Buhl, Y. J. Huang, C. O. Pedersen, R. K. Strand, R. J. Liesen, D. E. Fisher, M. J. Witte, et al. Energyplus: creating a new-generation building energy simulation program. *Energy and buildings*, 33(4):319–331, 2001.
- [15] G. Dulac-Arnold, D. Mankowitz, and T. Hester. Challenges of real-world reinforcement learning. *arXiv preprint arXiv:1904.12901*, 2019.
- [16] B. Foliaco, A. Bula, and P. Coombes. Improving the gordon-ng model and analyzing thermodynamic parameters to evaluate performance in a water-cooled centrifugal chiller. *Energies*, 13(9):2135, 2020.
- [17] G. Gao, J. Li, and Y. Wen. Energy-efficient thermal comfort control in smart buildings via deep reinforcement learning. *arXiv preprint arXiv:1901.04693*, 2019.
- [18] J. Gordon, K. C. Ng, and H. T. Chua. Centrifugal chillers: thermodynamic modelling and a diagnostic case study. *International Journal of refrigeration*, 18(4):253–257, 1995.
- [19] M. A. Hanif, F. Nadeem, R. Tariq, and U. Rashid. *Renewable and Alternative Energy Resources*. Academic Press, 2022.
- [20] V. Hanumaiah and S. Genc. Distributed multi-agent deep reinforcement learning framework for whole-building hvac control. *arXiv preprint arXiv:2110.13450*, 2021.

- [21] E. G. Hertwich, S. Ali, L. Ciacci, T. Fishman, N. Heeren, E. Masanet, F. N. Asghari, E. Olivetti, S. Pauliuk, Q. Tu, et al. Material efficiency strategies to reducing greenhouse gas emissions associated with buildings, vehicles, and electronics—a review. *Environmental Research Letters*, 14(4):043004, 2019.
- [22] M. Hoffman, B. Shahriari, J. Aslanides, G. Barth-Maron, F. Behbahani, T. Norman, A. Abdolmaleki, A. Cassirer, F. Yang, K. Baumli, S. Henderson, A. Novikov, S. G. Colmenarejo, S. Cabi, C. Gulcehre, T. L. Paine, A. Cowie, Z. Wang, B. Piot, and N. de Freitas. Acme: A research framework for distributed reinforcement learning. *arXiv preprint arXiv:2006.00979*, 2020.
- [23] H. Kazmi, F. Mehmood, S. Lodeweyckx, and J. Driesen. Gigawatt-hour scale savings on a budget of zero: Deep reinforcement learning based optimal control of hot water systems. *Energy*, 144:159–168, feb 2018.
- [24] B. S. Kim and A. J. Calise. Nonlinear flight control using neural networks. *Journal of Guidance, Control, and Dynamics*, 20(1):26–33, 1997.
- [25] D.-W. Kim and C.-S. Park. Difficulties and limitations in performance simulation of a double skin façade with energyplus. *Energy and Buildings*, 43(12):3635–3645, 2011.
- [26] F. Krausmann, C. Lauk, W. Haas, and D. Wiedenhofer. From resource extraction to outflows of wastes and emissions: The socioeconomic metabolism of the global economy, 1900–2015. *Global Environmental Change*, 52:131–140, 2018.
- [27] E. Liang, R. Liaw, R. Nishihara, P. Moritz, R. Fox, K. Goldberg, J. Gonzalez, M. Jordan, and I. Stoica. Rllib: Abstractions for distributed reinforcement learning. In *International Conference on Machine Learning*, pages 3053–3062. PMLR, 2018.
- [28] T. P. Lillicrap, J. J. Hunt, A. Pritzel, N. Heess, T. Erez, Y. Tassa, D. Silver, and D. Wierstra. Continuous control with deep reinforcement learning. *arXiv preprint arXiv:1509.02971*, 2015.
- [29] V. Mnih, A. P. Badia, M. Mirza, A. Graves, T. Lillicrap, T. Harley, D. Silver, and K. Kavukcuoglu. Asynchronous methods for deep reinforcement learning. In *International conference on machine learning*, pages 1928–1937. PMLR, 2016.
- [30] T. Moriyama, G. D. Magistris, M. Tatsubori, T.-H. Pham, A. Munawar, and R. Tachibana. Reinforcement learning testbed for power-consumption optimization. In *Asian simulation conference*, pages 45–59. Springer, 2018.
- [31] A. Muldal, Y. Doron, J. Aslanides, T. Harley, T. Ward, and S. Liu. dm_env: A python interface for reinforcement learning environments, 2019.
- [32] S.-H. Mun, J. Kang, Y. Kwak, Y.-S. Jeong, S.-M. Lee, and J.-H. Huh. Limitations of energyplus in analyzing energy performance of semi-transparent photovoltaic modules. *Case Studies in Thermal Engineering*, 22:100765, 2020.
- [33] Z. Nagy and K. Nweye. Real-world challenges for reinforcement learning in building control. *arXiv preprint arXiv:2112.06127*, 2021.
- [34] S. Narvekar, B. Peng, M. Leonetti, J. Sinapov, M. E. Taylor, and P. Stone. Curriculum learning for reinforcement learning domains: A framework and survey. *arXiv preprint arXiv:2003.04960*, 2020.
- [35] H. O. Portner, D. C. Roberts, H. Adams, C. Adler, P. Aldunce, E. Ali, R. A. Begum, R. Betts, R. B. Kerr, R. Biesbroek, et al. Climate change 2022: impacts, adaptation and vulnerability. 2022.

- [36] Y. Tassa, Y. Doron, A. Muldal, T. Erez, Y. Li, D. d. L. Casas, D. Budden, A. Abdolmaleki, J. Merel, A. Lefrancq, et al. Deepmind control suite. *arXiv preprint arXiv:1801.00690*, 2018.
- [37] A. Tortorelli, M. Imran, F. Delli Priscoli, and F. Liberati. A parallel deep reinforcement learning framework for controlling industrial assembly lines. *Electronics*, 11(4):539, 2022.
- [38] J. Wang, J. F. Rodrigues, M. Hu, P. Behrens, and A. Tukker. The evolution of chinese industrial co2 emissions 2000–2050: A review and meta-analysis of historical drivers, projections and policy goals. *Renewable and Sustainable Energy Reviews*, 116:109433, 2019.
- [39] X. Zhan, H. Xu, Y. Zhang, Y. Huo, X. Zhu, H. Yin, and Y. Zheng. Deepthermal: Combustion optimization for thermal power generating units using offline reinforcement learning. *arXiv preprint arXiv:2102.11492*, 2, 2021.
- [40] Z. Zhang, A. Chong, Y. Pan, C. Zhang, and K. P. Lam. Whole building energy model for hvac optimal control: A practical framework based on deep reinforcement learning. *Energy and Buildings*, 199:472–490, 2019.